Lessons in Nanotechnology from
Traditional and Advanced Ceramics
J.-F. Baumard (Editor)

ENGINEERING MULTILAYERED CERAMIC COMPOSITES AT THE NANOMETER SCALE TO ACHIEVE IMPROVED PROPERTIES

R. NASLAIN, R. PAILLER, X. BOURRAT,
S. BERTRAND, F. LAMOUROUX, A. FILLION
Laboratoire des Composites Thermostructuraux (LCTS), Université Bordeaux 1, Pessac, France

The engineering of non-oxide ceramic composites (mainly, fiber-reinforced and by extension, laminated and cellular) at a submicrometer scale (typically 10 to 100 nm) is discussed. Pressure-pulsed CVD/CVI is presented as a method of choice to fabricate these composites, at least at the laboratory or pilot-plant levels, with either a regular or graded composition and nanostructure. The oxidation resistance of non-oxide CMCs is improved through the development of a self-healing behavior, by reducing the thickness of the oxidation-prone layers (typically, the carbon or BN interphases) to 10-20 nm and introducing layers of materials forming healing oxides (such as boria or silica), namely, B_4C, SiB_6, SiC. The friction properties of C/C can be tailored by introducing nanosize layers of SiC in the matrix in a controlled manner: the coefficient of friction is increased but at the expense of wear resistance. Other properties, such as the thermal conductivity of SiC/SiC composites or their stability under nuclear radiations could also be tailored and improved through the engineering at a submicrometer scale of their constituents.

1. INTRODUCTION

Ceramic matrix composites (CMCs) are complex ceramic materials, mainly designed for structural applications at high temperature, and which may display outstanding properties when their composition, structure and texture have been properly tailored (or engineered), often at a submicrometer scale. Examples of these materials are ceramics - generally, non-oxides - consisting of a ceramic matrix reinforced with continuous ceramic fibers oriented in one single direction (1D-composites) or several directions (nD-composites with n = 2 or 3)[1-3], laminated ceramics made of a stack of tightly bonded layers of different nature or cellular ceramics[4-6]. Their most outstanding property lies in the fact that they can be *damage-tolerant* (or tough, with fracture energy of the order of 10 kJ/m^2), although their constituents are intrinsically brittle.

A classical way to achieve damage-tolerance in CMCs is to engineer the composite at an adequate scale in order that a crack initiated in the brittle main phase does not propagate in a catastrophic manner through the whole material (contrary to what is observed in monolithic ceramics) but is rather arrested or deflected with energy absorption by weak interphases or compliant phases. As an example, in fiber-reinforced CMCs, a thin layer of a compliant material with a low shear strength (such as an anisotropic pyrocarbon (or PyC), i.e. a sp^2 carbon deposited from a gaseous precursor, or a boron nitride), referred to as the *interphase*, is deposited on the fiber surface before the infiltration of the matrix, to arrest or/and deflect the matrix microcracks parallel to the fiber surface, hence protecting the fibers from an early failure by notch effect.

For this reason, it is sometimes called a "mechanical fuse" by analogy with the fuse commonly used to protect electrical circuits and devices[7, 8]. As a matter of fact, the interphase in CMCs often has a much complex function, also including load transfer, acting as diffusion barrier (in reactive fiber/matrix systems), absorbing at least partly the thermal residual stresses due to CTE (coefficient of thermal expansion) mismatch. Further, it should be chemically compatible with the fiber and matrix, as well as the environment. This last constraint is often crucial since most CMCs are non-oxides (for mechanical reasons, including strength at high temperature and creep resistance) and are used in corrosive oxidizing atmospheres (air or combustion gas). Other properties of CMCs, such as friction behavior (C/C and related C/C-SiC composites are materials of choice for braking systems)[9], thermal conductivity (in many applications, CMCs are used as thin parts submitted to transverse heat flux) or residual radioactivity after an irradiation in e.g. a fast neutron flux (high temperature fission or fusion nuclear reactors)[10], may also benefit from an engineering at an adequate scale.

The aim of the present contribution is to tentatively show, through selected examples taken from experimental and modelling studies conducted in recent years at LCTS or other laboratories : (i) what advantages could be expected from the engineering of CMCs at a submicrometer – not to say nanometer – scales, (ii) how such materials can be fabricated in a controlled and reproducible manner and finally, (iii) what are the related properties. It will be limited to *multilayered* ceramics, the case of composite ceramics based on nanoparticles being treated by other authors.

2. DESIGN AND PROCESSING TECHNIQUES

2.1. General considerations

Multilayered ceramics consist of ceramic layers with different composition that will be formulated as X and Y (such as X= PyC or BN and Y=

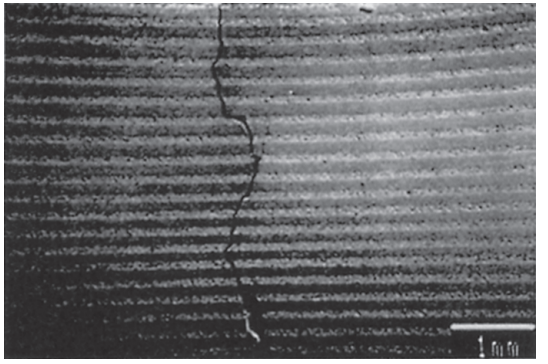

(a)

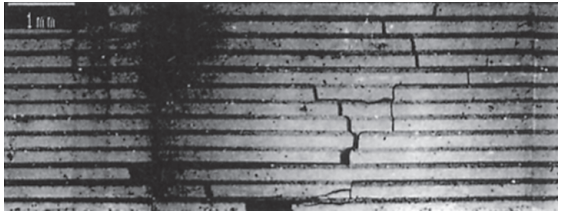

(b)

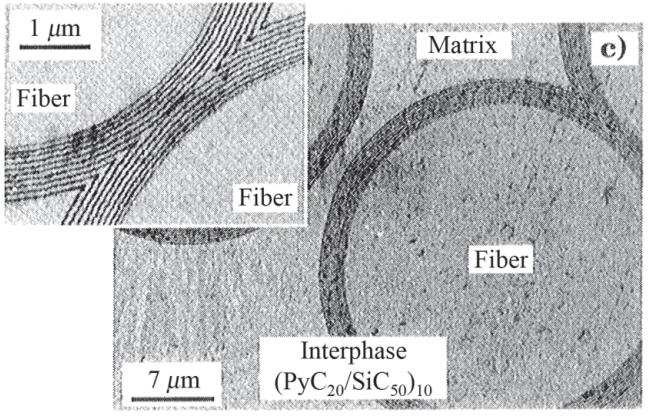

(c)

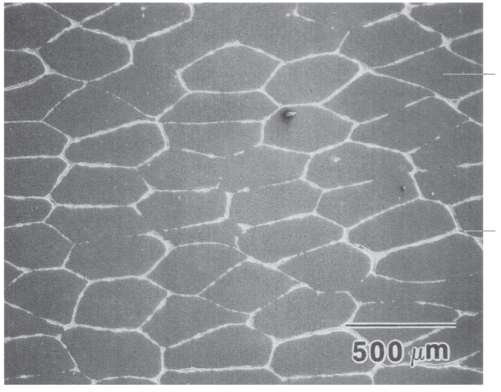

(d)

FIGURE 1 - Examples of damage-tolerant multilayered ceramics: (a), (b) alumina laminates with alternating dense and porous (Vp = 0.34 or 0.39) alumina layers, (c) 2D-SiC (Nicalon)/SiC composites with $(PyC\text{-}SiC)_{10}$ interphase and (d) cellular Si_3N_4-BN ceramics (adapted from ref. 4 (a, b), ref. 10 (c) and ref. 18 (d), respectively).

SiC) or different microstructure, referred to as X and X′, such as X for a dense phase and X′ for a porous layer, these two examples corresponding to two different classical concepts for achieving damage tolerance in CMCs. Hence, the multilayer can be written as $(X\text{-}Y)_n$ or $(X\text{-}X')_n$, where, n, is the number of elementary sequences which is repeated. Its overall thickness is given by:

$$e = \sum_{i}^{n} \left[e_i(X) + e_i(Y) \right] \quad \text{or} \quad e = \sum_{i}^{n} \left[e_i(X) + e_i(X') \right] \tag{1}$$

where $e_i(X)$, $e_i(Y)$ and $e_i(X')$ are the elementary thicknesses of the layers X, Y and X′ in the sequence of rank i. If the elementary thicknesses are constant, the multilayer has a *regular structure* and its overall thickness is now:

$$e = n[e(X) + e(Y)] \quad \text{or} \quad e = n[e(X) + e(X')] \tag{2}$$

However and as it will become apparent in some of the examples described in the following sections, e(X), e(Y) or/and e(X′) can be varied, yielding *graded multilayers* which display positive or negative composition or microstructure gradients and permit a broad range of material design that could be used to tailor a given property at different scales including the nanometer scale if the elementary thicknesses e(X), e(Y) or/and e(X′) can be reduced, by selecting an appropriate processing technique, to a few nm or 10 nm.

Multilayered ceramics can be fabricated by a variety of techniques, from slurries (sequencial tape casting, electrophoretic deposition or centrifugation, combined with a sintering step), sol-gels (dip-coating and sintering), sprays (sputtering or plasma spraying) or gaseous species (CVD, molecular beam epitaxy or MBE). Their processing is more or less straightforward depending on the shape of the multilayers and the scale at which it is designed. It is relatively easy for planar multilayers (all the techniques mentioned above can be used) but much more difficult when the multilayers have to be deposited inside a porous body, such as a nD-fiber preform, where a method of choice is the so-called *CVI-process* (for chemical vapor infiltration, a low temperature/pressure version of CVD). Further, the deposition in a controlled and reproducible manner of multilayers designed at a submicrometer scale is only possible with a few techniques, such as MBE, sol-gel or CVD/CVI. We will now depict with some details, the processing technique which has been developed at LCTS to deposit, on planar substrates or inside porous fiber architectures, ceramic multilayers engineered at the nm-scale, namely the *pressure-pulsed CVD or CVI* technique (P-CVD/CVI)[7-12].

2.2. Pressure-pulsed CVD/CVI

In *conventional CVD*, a solid is deposited from a gaseous precursor on a substrate heated at a given temperature T, in a cold or hot wall deposition chamber, through which the gaseous precursor is flowing under a constant pressure P and at a constant flow rate Q. Non-oxide ceramics, such as carbon, BN, SiC, B_4C or SiB_6, can be deposited from different gaseous precursors, according to the following overall equations:

$$2\,C_xH_{y\,(g)} \rightarrow 2xC_{(s)} + yH_{2\,(g)} \quad (3)$$

$$CH_3SiCl_{3\,(g)} \xrightarrow{H_2} SiC_{(s)} + 3HCl_{(g)} \quad (4)$$

$$4\,BCl_{3\,(g)} + CH_{4\,(g)} + 4\,H_{2\,(g)} \rightarrow B_4C_{(s)} + 12\,HCl_{(g)} \quad (5)$$

$$SiCl_{4\,(g)} + 6\,BCl_{3\,(g)} + 11\,H_{2\,(g)} \rightarrow SiB_{6\,(s)} + 22\,HCl_{(g)} \quad (6)$$

$$BX_{3\,(g)} + NH_{3\,(g)} \rightarrow BN_{(s)} + 3\,HX_{(g)} \quad \text{with X = F, Cl} \quad (7)$$

The deposition rate depends on the three T, P, Q parameters as well as the nature and composition of the gaseous precursor. When deposition occurs on the external surface of a substrate (CVD), the deposition parameters can be varied within large domains (the deposition rate, R, increasing when T, P, Q are raised). Conversely, in *conventional CVI* used to densify porous bodies, such as a fiber preform, deposition should preferentially occur inside the substrate pore network, in order to prevent the early sealing of the pore entrances by the deposit. This is achieved by lowering the T, P parameters in such a way that the kinetics of deposition is slow – and therefore rate controlling – with respect to the mass transfer of the reactants and reaction products in the pore network by diffusion. As an example, the infiltration of pyrocarbon and BN (both used as interphases or cell boundaries in non-oxide composites), on the one hand, and that of SiC, B_4C or SiB_6 (matrix constituents), on the other hand, according to equations (3) to (7), are usually conducted at $900 < T < 1100$ °C and under a pressure of a few kPa or 10 kPa[13].

In *pressure-pulsed CVD/CVI*, the reactants are injected in the deposition chamber, which has been previously evacuated with a rotary pump, in a very short time, t_a (typically, a fraction of a second: 0.1 to 0.3 s), the pressure reaching a preset value P. Then, the deposition chamber is isolated (inlet and outlet valves closed) and deposition occurs during a preset time, t_d, which is of the order of a few seconds or less. Finally, the deposition chamber is evacuated by pumping during a short time, t_p, also of the order of a fraction of a second, and eventually maintained under vacuum during a time, t_v. The elementary injection – deposition – evacuation sequence is automatically repeated versus time, with pneumatic valves monitored with an automation device (Fig. 2) [7, 8, 10-12].

P-CVD/CVI display two important advantages. Firstly, the deposition rate,

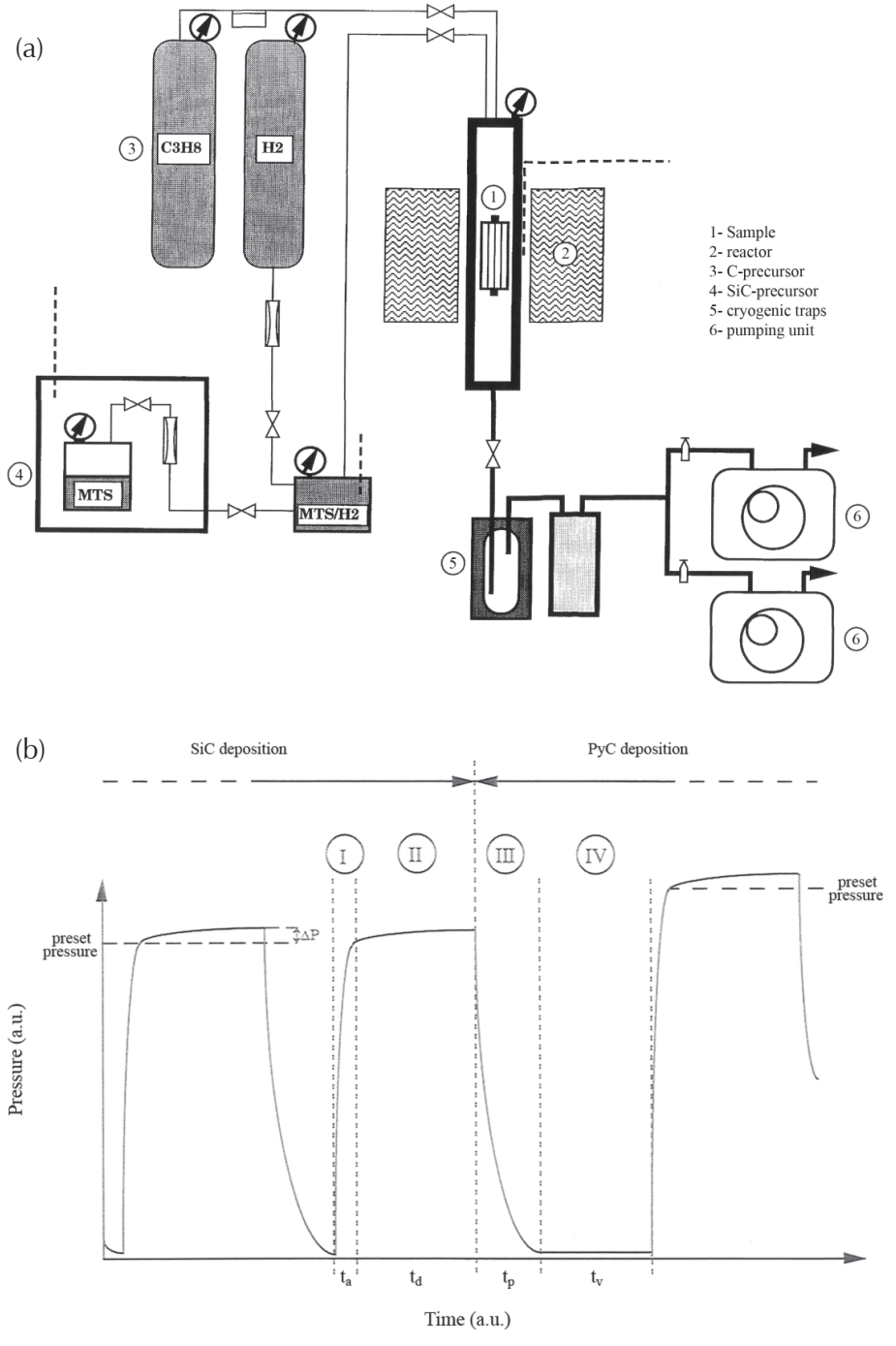

FIGURE 2 - The pressure-pulsed CVD/CVI processing technique: (a) example of experimental set-up for the deposition of (PyC-SiC)$_n$ multilayers and (b) related P-pulses (adapted from ref. 10 and 8 respectively).

R, is high since deposition occurs from fresh reactants and reaction products (which often act as deposition inhibitors) are periodically evacuated. Secondly and more importantly here, multilayered $(X\text{-}Y)_n$ deposits, such as $(PyC\text{-}SiC)_n$, can easily be deposited if the nature of the gaseous precursor is periodically changed (switching, in this example, from a hydrocarbon, C_xH_y (equation 3), to a mixture of methyltrichlorosilane (MTS) and hydrogen (equation 4)). The X-layer being formed of N(X) elementary films of thickness e_p (X) and that of Y of N(Y) elementary films of thickness e_p(Y), the overall thickness of the multilayer, is given again by equation (1), rearranged as:

$$e = \sum_{i}^{n} \left[e_p(X) N_i(X) + e_p(Y) N_i(Y) \right] \qquad (1')$$

where n is the number of elementary X-Y sequences, N_i (X) and N_i (Y) the numbers of P-pulses used to deposit the X and Y layers in the X-Y sequence of rank i. If the multilayer is designed to be *regular*, the numbers of P-pulses and the preset values of t_d for X and Y remain constant and equation (2) can be written as:

$$e = n[e_p(X)\, N\,(X) + e_p\,(Y)\, N\,(Y)] \qquad (2')$$

Conversely, multilayers with graded composition or/and microstructure are formed if the P-pulse numbers (and hence the layer thicknesses) are changed versus time, as deposition proceeds. Finally, the multilayers can be engineered at the *nanometer scale* (with X and Y-layer thicknesses of the order of a few nm to a few 10 nm), by : (i) lowering the deposition rates *per pulse*, e_p(X) and e_p(Y) which depend on the deposition kinetics and hence the preset T, P values, as well as the deposition duration, t_d and (ii) decreasing the numbers of P-pulses, N_i(X) and N_i(Y) per sequence. As a matter of fact, the deposition rate is not uniform in a P-pulse : it is high at the beginning of a pulse and then it decreases as the reactants are consumed and the reaction products formed, a feature which justifies the use of short P-pulses (typically, one to a few seconds). Consequently, the thickness of X and Y deposited per P-pulse, in equation (1') and (2'), should be written as:

$$e_p(X) = \int_{o}^{t_d(X)} R_X\, dt \qquad \text{and} \qquad e_p(Y) = \int_{o}^{t_d(Y)} R_Y\, dt \qquad (8)$$

where R_X and R_Y are the "instantaneous" deposition rates of X and Y.

Hence, it clearly appears that P-CVD/CVI can be a very suitable way to deposit multilayered ceramics, engineered at the nm-scale when necessary, either on the external surface of a substrate (P-CVD) or more interestingly

here, within its open pore network (P-CVI) in a controlled and reproducible manner (the adjustable parameters being T, P, $t_d(X)$, $t_d(Y)$, N(X), N(Y)) and n, as it will become apparent through the following selected examples.

3. NON-OXIDE CMCs WITH IMPROVED OXIDATION RESISTANCE

3.1. General considerations

3.1.1. Non-oxide fiber-reinforced, laminated and cellular ceramics are intrinsically oxidation-prone. When exposed to an oxidizing atmosphere, their constituents undergo *active or passive* oxidation depending on whether the oxidation products are totally gaseous or partly condensed, respectively. Carbon, from the fibers, the interphases or the cell boundaries undergoes exclusively active oxidation at temperature beyond about 500 °C, according to the following overall equations :

$$C_{(s)} + O_{2(g)} \rightarrow CO_{2(g)} \quad (9)$$

or $$C_{(s)} + \tfrac{1}{2}\, O_{2(g)} \rightarrow CO_{(g)} \quad (9')$$

BN, which is mainly used as interphase or cell boundary, has a better oxidation resistance since its oxidation in dry atmospheres starts at about 700°C and yields an oxide, B_2O_3, which remains liquid up to about 1100 °C :

$$2\, BN_{(s)} + 3/2\, O_{2(g)} \rightarrow B_2O_{3(s,\,l)} + N_{2(g)} \quad (10)$$

However, this is no longer true when the oxidizing atmosphere contains water vapor at high water vapor partial pressure. Under such conditions, boria reacts with water, even at low temperature, to yield gaseous species, such as HBO_2, according to:

$$B_2O_{3(l)} + H_2O_{(g)} \rightarrow 2\, HBO_{2(g)} \quad (11)$$

Conversely, all the other constituents (mainly present in the matrix) undergo passive oxidation, in a broad range of oxidation conditions :

$$SiC_{(s)} + 2\, O_{2(g)} \rightarrow SiO_{2(s)} + CO_{2(g)} \quad (12)$$

or $$SiC_{(s)} + 3/2\, O_{2(g)} \rightarrow SiO_{2(s)} + CO_{(g)} \quad (12')$$

$$B_4C_{(s)} + 7/2\, O_{2(g)} \rightarrow 2\, B_2O_{3(l)} + CO_{(g)} \quad (13)$$

$$SiB_{6(s)} + 11/2\, O_{2(g)} \rightarrow SiO_{2(s)} + 3\, B_2O_{3(l)} \quad (14)$$

The condensed oxides (silica or/and boria) are protective. They are formed with volume expansion and characterized by a low coefficient of diffusion for oxygen. However, under specific conditions, such as very high temperature and low oxygen partial pressure (encountered by spacecraft in earth atmosphere re-entry), the oxidation regime of Si-bearing phases may become active, the protective condensed oxides being no longer formed :

$$SiC_{(s)} + O_{2(g)} \rightarrow SiO_{(g)} + CO_{(g)} \quad (15)$$

In terms of oxidation resistance, CMCs have two weak points, namely the fibers (both carbon and SiC-based fibers are weakened by oxidation with a strength which can be dramatically degraded) and the interphases (PyC or BN) whose oxidation alters or even destroys the fiber-matrix (FM) coupling (and hence the load transfer function).

3.1.2. The oxidation resistance of non-oxide CMCs can be improved by promoting the so-called mechanisms of *self-healing* in the materials when exposed to an oxidizing atmosphere[14-17]. As schematically shown in Fig. 3a (for a 1D-SiC_f/C/SiC_m or more simply 1D-SiC/C/SiC with a pyrocarbon interphase, submitted to an oxidation test in the fiber direction), the oxidation of the carbon interphase forms an annular pore around each fiber whose length, L_R, increases versus time. As a result, oxygen has now to diffuse along that pore to react with the interphase. During that diffusion, it can also react with the pore walls (the SiC-based fiber and the matrix), yielding two silica scales whose thicknesses are larger near the pore entrance (where the atmosphere is oxygen-rich) than in-depth in the pore, and increase versus time. If the oxidation conditions are appropriate, these silica scales can plug the pore entrance (the pore becoming sealed by silica), slowing down (not to say almost stopping) the in-depth oxygen diffusion and the related gasification of the interphase. The material is said to display a *self-healing* behavior. All these phenomena can be modelled for the simple 1D-composite shown in Fig. 3a (on the basis of the diffusion equations, the kinetic laws and appropriate boundary conditions)[14, 15]. Among others, the model gives the length of carbon interphase, L_R, which is consumed by oxidation versus time, as well as the time necessary for pore sealing, for a given test temperature, O_2-partial pressure and interphase thickness, e(PyC). As shown in Fig. 3 b,c, the pore is practically never sealed at low temperatures (typically, 900°C) when the interphase is relatively thick (e(PyC) = 100 nm or more). Under such unfavorable conditions, the formation of the silicon healing oxide is too slow with the result that oxidation proceeds in-depth with a degradation of the FM-bonding and mechanical properties. Conversely, at high temperatures (say, 1200-1300 °C) and for extremely thin PyC-interphase (50 nm or less), the pore sealing occurs

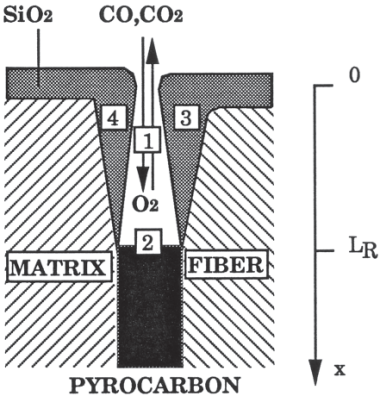

(a)

1 - in-depth diffusion along annular pore
2 - reaction of oxygen with PyC-interphase
3, 4 - reaction of oxygen with pore walls

(b)

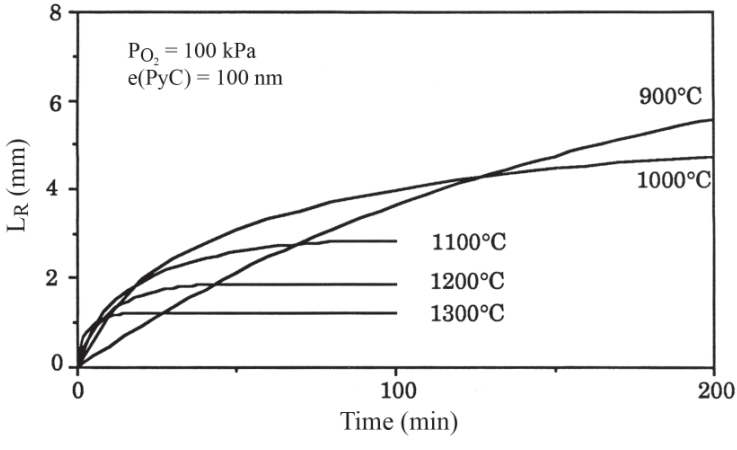

(c)

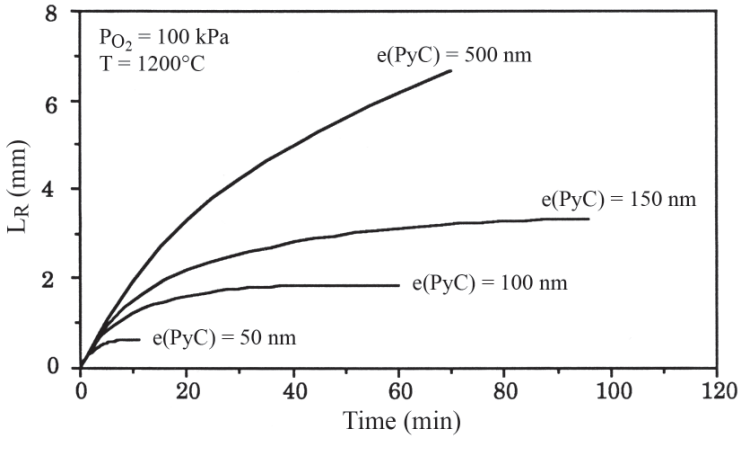

FIGURE 3 - Oxidation of a model 1D-SiC/C/SiC composite in the fiber direction: (a) basic phenomena, (b, c) length of PyC interphase consumed vs time as a function of temperature and PyC-interphase thickness (adapted from ref. 14).

in a very short time since the kinetics of silica growth is now fast and the pore to be filled is narrow.

Hence, three conditions should be *simultaneously* fulfilled to give a self-healing character and good oxidation resistance to non-oxide ceramics (either laminated, cellular or fiber-reinforced). Firstly, the oxidation-prone phase, i.e. the mechanical fuse for crack deflection, should be as thin as possible. In other words, the material should be designed at the *nanometer scale*. Secondly, the matrix microcracks when they form under load, should be as narrow as possible (a narrow crack being easier to fill than a widely open crack), which is actually observed, in fiber-reinforced composites, when the FM-bonding is not too weak (under such conditions, the matrix crack density is high but the cracks are individually narrow). Thirdly, the oxidation kinetics of the healing oxide former should be fast at the test temperature, which is the case for SiC beyond $\approx$ 1000 °C but not at lower temperatures.

The self-healing material concept has been successfully applied to non-oxide fiber-reinforced composites (and could also be extended to laminated or cellular ceramics), through a material design at the nm-scale and a fabrication by P-CVI, at the levels of both the interphase and the matrix.

3.2. Non-oxide CMCs with a multilayered interphase designed at the nanometer scale

Fig. 4 shows TEM-images of $(PyC\text{-}SiC)_n$ multilayered interphases in 2D-SiC (Nicalon)/SiC and 1D-SiC (Hi-Nicalon)/SiC composites designed at the nanometer scale and fabricated by P-CVI (Nicalon and Hi-Nicalon are SiC-based fibers from Nippon Carbon, Japan)[10]. In both cases, n = 10, e(PyC) = 20 nm and e(SiC) = 50 nm. It clearly appears that the morphology of the multilayers is very regular even though they were deposited in the pore network of fiber architectures (a stack of fiber fabrics and a fiber tow, respectively), a feature which demonstrates the potential of the P-CVI processing technique. This was achieved through a proper selection of the deposition conditions. The pyrocarbon layers were deposited from propane, with the graphene planes parallel to the fiber surface, at least in a first approximation[7]. The SiC-based layers were deposited from a MTS-rich MTS/H_2 mixture. Under such conditions, they consist of a SiC + C mixture and are nanocrystallized (whereas stoichiometric SiC-layers would display facetted SiC-grains of relatively "large" size resulting in rough PyC/SiC interfaces)[8, 10].

1D-SiC (Hi-Nicalon)/$(PyC\text{-}SiC)_{10}$/SiC composites display at room temperature, a non-linear mechanical behavior under tensile loading, similar to that of their counterpart with a single layer pyrocarbon interphase (e(PyC) = 100 nm). As shown in Fig. 4, the matrix cracks are deflected in the interphase, mainly at the level of each pyrocarbon layer, a feature which demonstrates

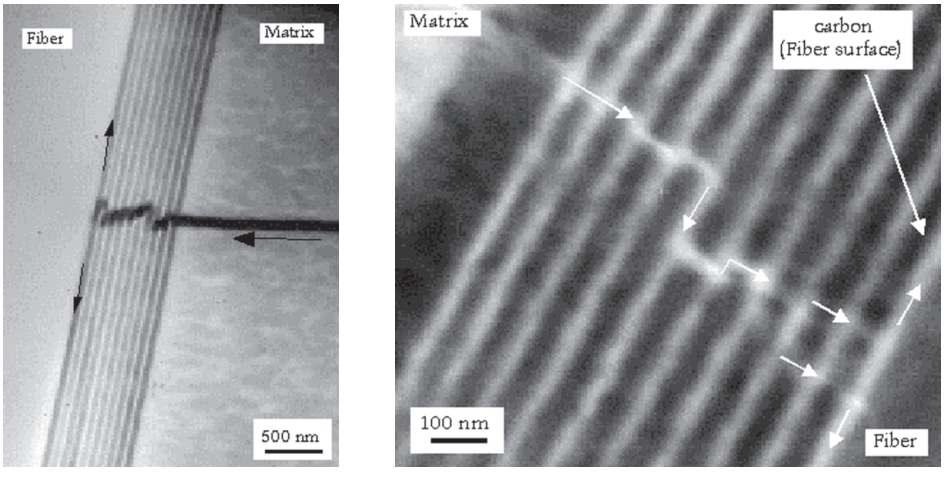

(a) (b)

FIGURE 4 - TEM images of $(PyC\text{-}SiC)_{10}$ multilayered interphases in: (a) 2D-SiC (Nicalon)/SiC composite and (b) 1D-SiC (Hi-Nicalon)/SiC model minicomposite, both engineered at the nm-scale and deposited by P-CVI (adapted from ref. 10).

that a thin pyrocarbon layer, i.e. only 20 nm thick, can still act efficiently as mechanical fuse, justifying the interphase design at the nanometer scale. Further and as expected from the discussion presented in section 3.1.2, replacing the relatively thick (100 nm) single pyrocarbon interphase by a multilayer in which the thickness of the elementary pyrocarbon layers is reduced to 20 nm, improves the oxidation resistance of the composite when exposed to an oxidizing atmosphere under load. As an example, the lifetime in air at 700 °C under tensile static fatigue loading slightly above the proportional limit (which is the onset of matrix microcracking), increased from 100 to 150 hours when the single 100 nm-thick pyrocarbon interphase was replaced by the multilayered interphase[10]. This significant gain in lifetime (50%) could result from: (i) the reduction of the PyC-layer thickness itself from 100 to 20 nm (see Fig. 3b) and (ii) the longer crack propagation path (see Fig. 4b), both rendering easier the healing of the narrower cracks, even though the formation of silica is slow at this temperature. A similar conclusion was reported for composites with $(BN\text{-}SiC)_n$ multilayered interphases (with n = 10, e(BN) = 40 nm and e(SiC) = 25 nm), lifetime increasing from 45 to 140 hours (210%) when the single 150 nm –thick BN-interphase was replaced by the multilayered interphase (even though in this case, the FM-bonding was not optimized and still better results, in terms of lifetime, expected)[10].

From the results reported above, the question is now: could the multilayered interphase design be extended to a lower scale or in other words

what is the lower limit for the mechanical fuse layer thickness. The answer to that question is still a matter of speculation. Interestingly, in a study on 2D-SiC(Nicalon)/SiC composites with $(PyC\text{-}SiC)_{10}$ multilayered interphases, it was found that the composite with e(PyC) = 3 nm (only 10 graphene atomic planes) and e(SiC) = 10 nm failed at a low strain (≈ 0.3%) and displayed a very short lifetime in cyclic tensile loading at either 600 or 1200°C in air, whereas that with e(PyC) = 20 nm and e(SiC) = 50 nm failed at a much higher strain (≈ 0.8%) with an extended non-linear domain, and exhibited under the same conditions an improved lifetime with respect to the material with a single 100 nm thick interphase[10]. Hence, it could be anticipated that there is actually a lower limit for the thickness of the mechanical fuse layer, which could be of the order of e(PyC) = 10-20 nm for the fibers considered here. This limit is thought to depend upon the roughness of the X-SiC interfaces (and that of the fiber surface). Below this limit, the roughness of these interfaces permits direct and strong local bonding between the SiC-layers that embrittles the composite, the discontinuous ultra thin X-layers no longer acting as mechanical fuses. It is worthy of note that in 1D-SiC (Hi-Nicalon)/$(BN\text{-}SiC)_{10}$/SiC composites, the crystallization state of the SiC-layers (beyond the second layer) is higher and higher as n increases, which results in rougher BN/SiC interfaces. Hence, the BN-layer thickness has to be set to e(BN) = 25 or 40 nm (without being yet optimized) to achieve a well developed damage-tolerance character. It is anticipated that in such a case, the lower limit of e(BN) might be higher than for the related $(PyC\text{-}SiC)_n$ multilayered interphases[10].

The discussion presented above for non-oxide fiber-reinforced composites, in terms of damage tolerance and oxidation resistance, could be extended in principle to 2D-ceramic laminates[4-6] as well as to 3D-cellular ceramics[18, 19]. In all these materials, damage tolerance is similarly achieved through the use of thin layers of mechanical fuse for crack deflection, which are typically layers of pyrocarbon or BN for SiC-based ceramics and BN-layers for silicon nitride. Although these ceramics are presently designed at the micrometer scale, there might be an advantage, particularly in terms of oxidation resistance, in reducing the thickness of the mechanical fuse layers (in laminates) or cell boundaries (in cellular ceramics), with the same questions about the occurrence of a thickness lower limit and the related role played by the layer (or cell) roughness. More research in this direction would be appropriate.

3.3. Non-oxide CMCs with a multilayered self-healing matrix designed at the nanometer scale

The concept of self-healing multilayered material depicted previously for the interphase in non-oxide CMCs has been successfully extended, in a

second step, to the matrix itself. Namely, the matrix instead of being a homogeneous single phase, say SiC or Si_3N_4, is now a multilayer, with mechanical fuse layers (X) for crack deflection and layers of materials (Y) forming healing oxides (such as silica or fluid boria) when exposed in a given temperature range, to an oxidizing atmosphere, with two important advantages. Firstly, the matrix cracks being now deflected in the matrix itself, their propagation paths – along which oxygen can be entrapped in condensed oxides – are much more extended, namely, at the micrometer- not to say millimeter – scales. Secondly, oxygen is entrapped far from the oxidation-prone interphases and fibers, reducing thus the risk of mechanical degradation of the materials. Finally, such matrices gain in being designed at the nanometer scale to enhance the healing efficiency, as discussed previously for the interphases.

An example of a non-oxide *model* CMC with a multilayered self-healing $(X\text{-}Y\text{-}X\text{-}Y')_n$ matrix is shown in Fig. 5[9]. This matrix, designed at the nanometer scale and infiltrated by P-CVI either in a fiber tow or a 2D fiber preform, is highly engineered. It consists of PyC-based X-layers (mechanical fuse function) and two different healing oxide formers active in complementary temperature ranges, Y = B_4C and Y′ = SiC (equations 12 and 13), with n = 4. These layers were deposited according to the overall equations (3), (5) and (4),

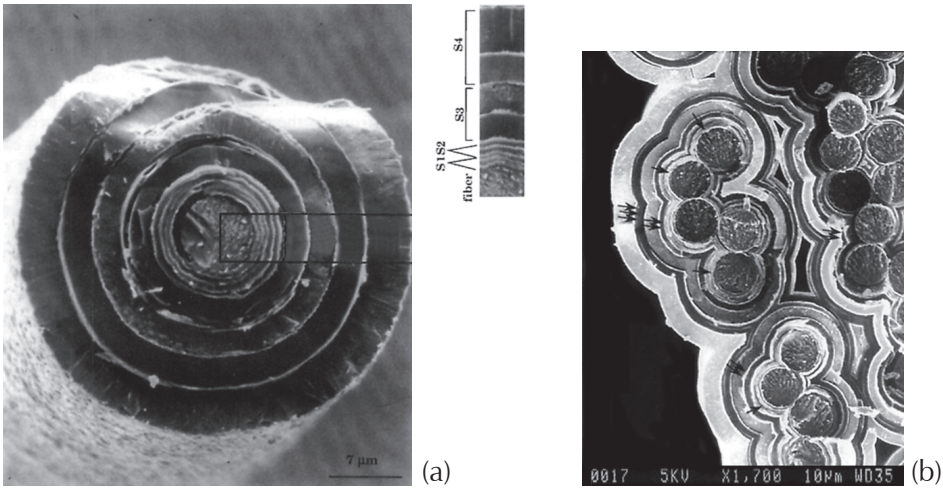

(a) (b)

FIGURE 5 - An example of self-healing multilayered matrix designed at the nanometer scale and deposited in a fiber tow by P-CVI: (a) the elementary S_1 to S_4 sequences as deposited on a single fiber in the tow and (b) viewed on a tow cross-section (adapted from ref. 9).

respectively. Further, the overall thickness of a given X-Y-X-Y' sequence progressively increases when moving apart from the fiber substrate. Those of the two first sequences (S1 and S2) were intentionally limited in order that each fiber was individually protected (single arrows in Fig. 5b) whereas the third (S3) and fourth (S4) sequences were thicker, to surround groups of fibers (double arrows) and finally the whole fiber tow (triple arrows) and enhance the self-healing behavior. Hence, the multilayered matrix both exhibits composition and morphology gradients, each X, Y, and Y' layer being deposited from P-pulses of increasing numbers N(X), N(Y) and N(Y') as n increases.

Composites with such a tailored matrix display two interesting properties related to their nanostructure. Firstly, their oxidation resistance is significantly improved with respect to the composite with a uniform SiC-matrix. As an example, the lifetime at 600 °C in air under static fatigue loading (4-point bending at a stress level close to the proportional limit) of a 2D fiber composite with a matrix similar to that shown in Fig. 5 was reported to increase by more than one order of magnitude with respect to the composite with a homogeneous SiC-matrix and SiC-seal – coating [9]. Secondly, 1D-carbon fiber model composites with such a matrix were not microcracked in the as-processed state (microcracking being systematically observed in C/SiC composites due to CTE-mismatch). In other words, a multilayered matrix properly designed and fabricated at the nanometer scale can absorb the thermal stresses arising form CTE-mismatch during cooling (FGM-concept).

This second example shows again the benefit that one could gain in designing multilayered matrices of non-oxide CMCs at the nanometer scale, from fundamental and applied standpoints.

4. NON-OXIDE CMCs ENGINEERED AT NANOMETR SCALE TO TAILOR THEIR FRICTION PROPERTIES

4.1. General considerations

Fiber-reinforced C/C composites are extensively used in braking systems of aircraft and racing cars. With respect to steel brakes, they are lighter, they can be used in a larger temperature range and they display better mechanical and tribological properties at high temperature, with an improved lifetime. By contrast, C/C are oxidation-prone and their friction behavior is altered at low temperatures in wet atmosphere. It has been recently suggested to replace part of the C-matrix by SiC to improve the oxidation resistance and the friction properties at low temperatures. C/C-SiC (Si) composites have been fabricated from 2D-carbon fiber preforms, first consolidated with carbon and then infiltrated with liquid silicon at 1400-1600 °C, according to the so-called RMI (reactive melt infiltration) or LSI (liquid silicon infiltration) process, silicon

reacting with carbon to form a SiC-based matrix containing a significant amount of free-silicon and referred to as SiC (Si). Finally, the material was coated with a SiC-based coating, actually being the friction surface. They were reported to display a very low wear rate W_R (when sliding against organic or metallic pad materials) and a high coefficient of friction, μ, almost insensitive to moisture at service temperatures[20, 21].

A series of C/C-SiC model composites has been fabricated at LCTS by a totally different technique, in order to tentatively work out the effect of small amounts of SiC added to the carbon matrix, on the bribological behavior of the material *sliding against itself* with no SiC-coating, the C-SiC matrix being engineered at the nanometer scale to spread the SiC-addition in the pyrocarbon phase in different manners[12].

4.2. C/C-SiC composites with a matrix engineered at the nanometer scale

In terms of material design, one or several thin layers of SiC were introduced in the pyrocarbon matrix, as schematically shown in Fig. 6, corresponding to a volume fraction ranging from 0.4 to 6.2% (or from 0.7 to 9.4 wt.%). The 3D-fiber preform consisted of 0° ± 60° ex-PAN carbon fiber unidirectional layers needled in the Z-direction (perpendicular to the layers stack). The matrix constituents were deposited by P-CVI at about 1000 °C from a MTS/H_2 gaseous mixture for SiC-layers and mainly from toluene for pyrocarbon. SiC was deposited either as a single layer (100 – 170 nm thick) at different distances from the fiber surface or as 3 to 15 discrete layers, to study the effect of the SiC-distribution mode on the tribological behavior. As an example, the deposition of the C-SiC matrix for the CCS3-sample (with 3 SiC layers and corresponding to the highest value of V_{SiC}) required a total of 141,500 P-pulses (113,500 toluene pulses with t_d = 0.8 s for PyC 1 and t_d = 2s for the following PyC-deposits, and 28,000 MTS/H_2 pulses with t_d = 1 s for the SiC-layers), corresponding to an overall true deposition time (not including the cumulated injection and evacuation steps) of ≈ 70 hours.

This new example shows, in a different field, the versatility of the P-CVI process to engineer complex matrices at a submicrometer scale, in an efficient and elegant way, at least at the laboratory scale. Further, the elementary thickness of the SiC-layers could have been reduced to a lower scale since the number of P-pulses, N(SiC), for the thinnest layers deposited in the present study was N(SiC) = 1800 with t_d = 1s, for the CCS15 sample. However, this would have required different deposition conditions, in order to smooth the SiC-layer morphology, i.e. to avoid the growth of facetted crystals, as discussed previously. Finally, Fig. 7 shows representative SEM-images of the C/C-SiC model composites[12].

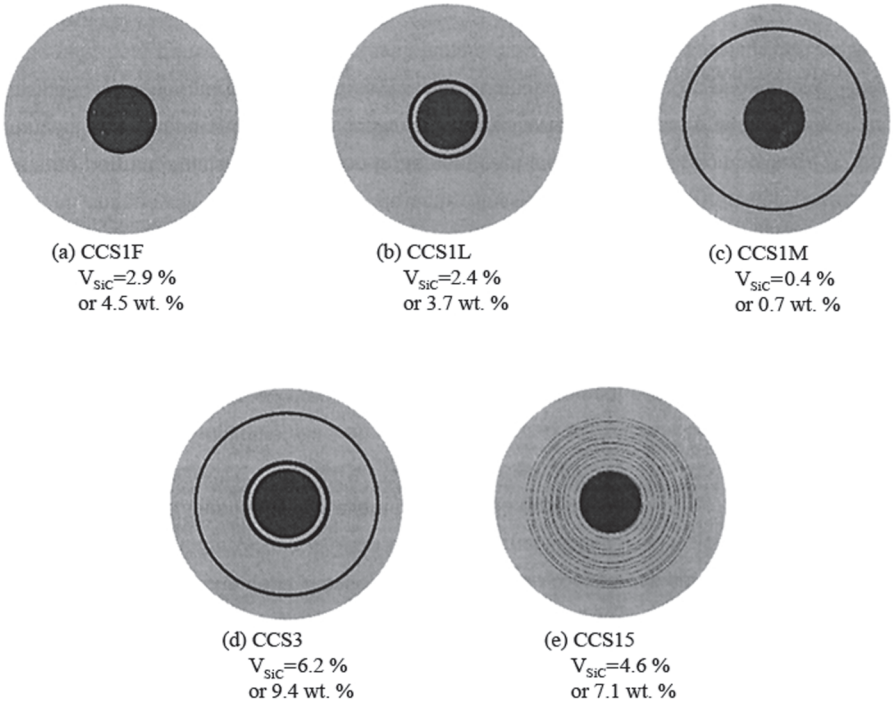

FIGURE 6 - Different C-SiC matrices engineered at a submicrometer scale (schematic): (a) one single 150 nm SiC layer deposited on the carbon fiber, (b) one single 170 nm SiC layer at 280 nm from fiber surface, (c) one single 100 nm SiC layer at 6 μm from fiber surface, (d) 3 SiC layers with thicknesses and location similar to those in (a) to (c) and (e) 15 discontinuous SiC layers spread over 5 μm (adapted from ref. 12).

4.3. Tribological properties

Generally speaking, C/C composites are known to display two different friction regimes : a regime of low coefficient of friction ($\mu \approx 0.1$) and a regime of high coefficient of friction ($\mu \approx 0.3$), the transition between them depending on different parameters including : sliding velocity (V_s), applied pressure (σ_R), temperature (T) and atmosphere. It is admitted that the high μ-regime is related to interactions between the dangling bonds formed at the edges of the graphene layers (active sites) in the interfacial zone during frictional sliding, whereas the low μ-regime corresponds to the de-activation of the active sites by chemisorption of water, oxygen or hydrogen. Increasing temperature contributes to desorb these species and increasing sliding velocity favors the formation of debris and new dangling bonds in the contact, both inducing the transition between the low and high μ-regimes.

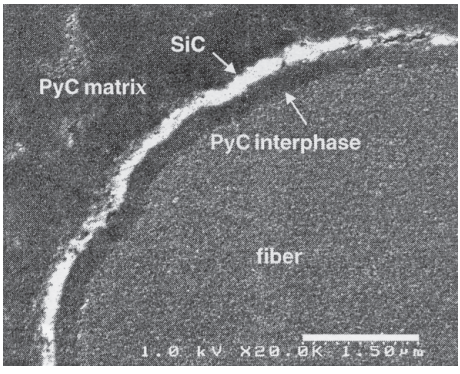

(a) CCS 1L

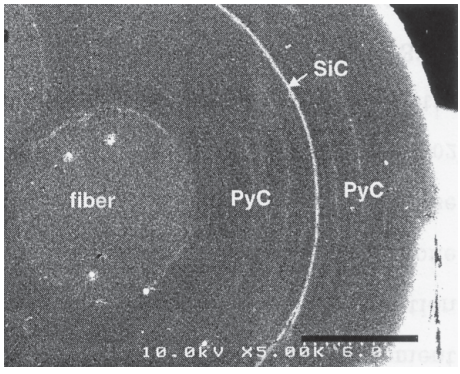

(b) CCS 1M

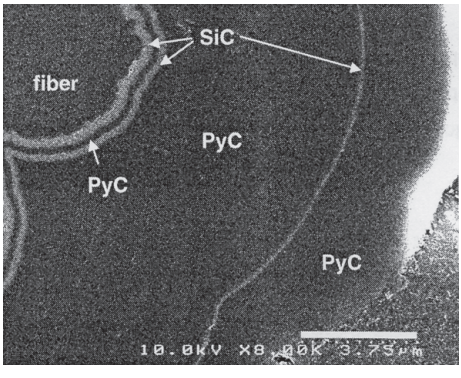

(c) CCS 3

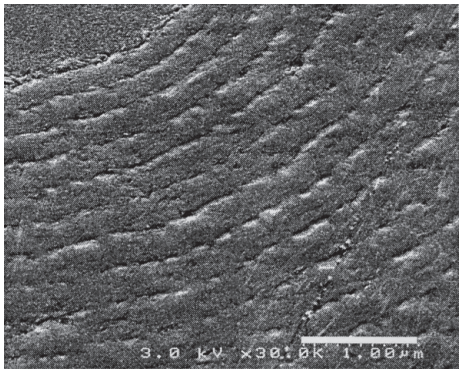

(d) CCS 15

FIGURE 7 - SEM images of different C/C-SiC model composites fabricated by P-CVI from 2D-ex-PAN carbon fiber preforms (adapted from ref. 12).

For the purpose of comparison, both the C/C and related C/C-SiC model composites have been submitted to tribological tests (configuration: pin sliding on a rotating disk of same nature)* under conditions assumed to correspond to the high-μ regime, namely, T = 200 °C, s_R = 3.5 MPa and V_S = 0.15 to 0.3 $m.s^{-1}$. They were performed under argon or dry air atmospheres on the as-infiltrated composites, to take into account the specific properties of pyrocarbon deposited from toluene[12].

The main results of this preliminary study are shown in Fig. 8 and could be tentatively summarized as follows. Firstly, in dry air, the coefficient of friction does not change markedly ($\mu \approx 0.25$) as long as the SiC-content of the composite

** tests performed at CNRS-ICS, Mulhouse, France*

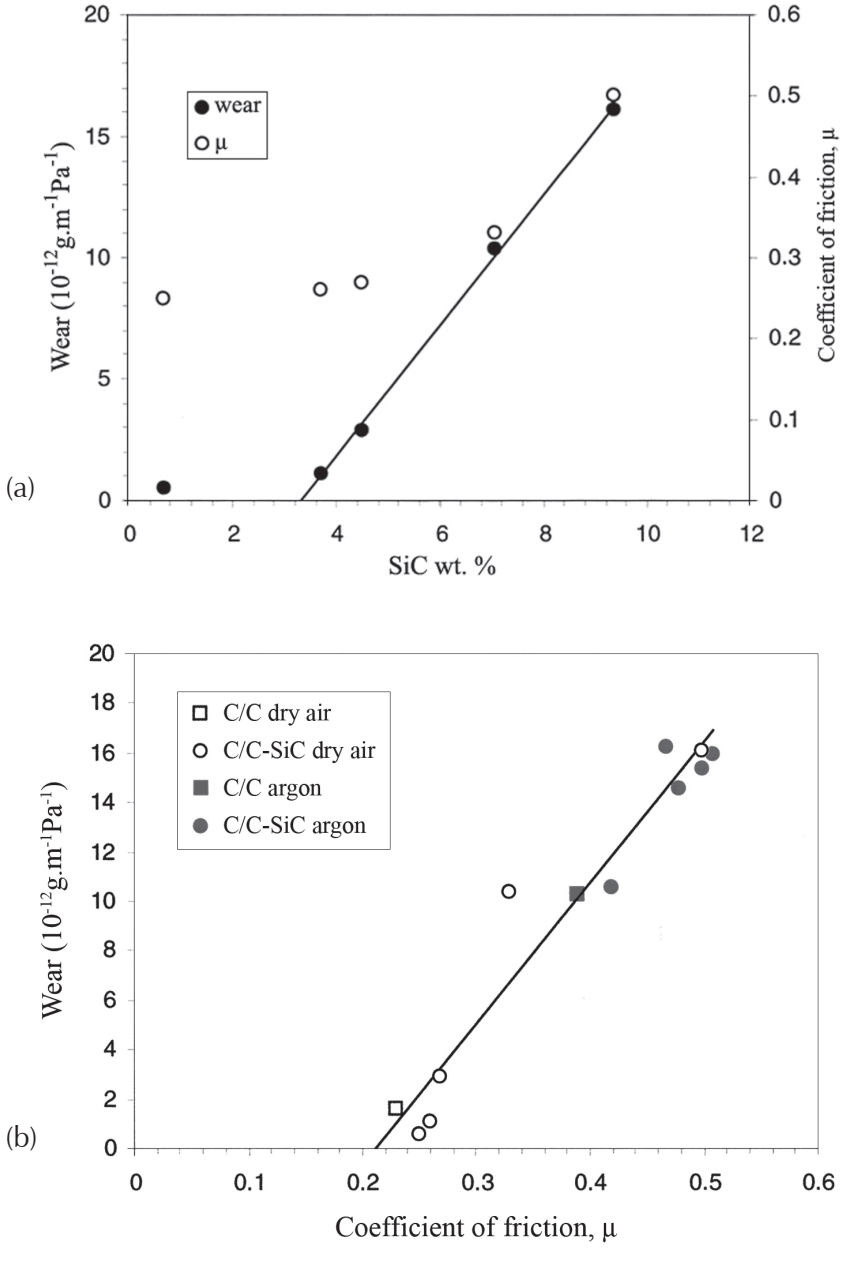

FIGURE 8 - Tribological properties (pin on disk configuration) of C/C-SiC model composites engineered at a submicrometer scale and fabricated by P-CVI: (a) variations of coefficient of friction and wear as a function of SiC wt. % (dry air; 200 °C; 3.5 MPa; 0.15 m s^{-1}) and (b) linear relationship between wear and coefficient of friction in C/C and related C/C-SiC composites tested in dry air or argon (200 °C; 3.5 MPa; 0.15 and 0.3 m s^{-1}) (adapted from ref. 12).

remains below 4-5 wt.% (or 0.4 to 2.9 vol.%) for the materials with one single SiC-layer (with e(PyC) ranging from 100 to 170 nm). Further, the localization of the SiC-layer(s) does not seem to play a key role: (i) the three samples with one single SiC-layer exhibit almost the same μ-values although the localization of the SiC-layer is very different, (ii) the coefficient of friction of the composite with 15 discontinuous ultra thin SiC-layers spread over 5 μm is indeed lower than that of the material with only 3 continuous SiC-layers, but its SiC-content is also lower (7.1 vs 9.4 wt. % or 4.6 vs 6.2 vol. %). The dominant parameter might well be the *overall SiC content*. Hence, introducing some SiC in the pyrocarbon matrix, even in relatively modest proportion, significantly increases the coefficient of friction (from 0.2 to 0.5 in dry air for only 6.2 vol. % (or 9.4 wt. %) which was the expected (and positive) effect. Interestingly, this effect is more limited under argon since the μ-value of the C/C composite is already high (μ only increasing here from 0.4 to 0.5 for the same SiC-addition). Secondly, the increase in μ is unfortunately associated – almost in a perfect linear relationship – with an *increase in wear* (obviously, an undesirable feature)[12].

The occurrence of SiC, a very hard phase compared to the relatively soft pyrocarbon matrix, is responsible for the continuous formation of debris and hence new dangling bonds in the pyrocarbon phase, even when present in modest proportion in the contact, which might explain the high observed μ-values. Further, its abrasive character also probably justifies the high wear, with respect to the very low wear rate previously reported for C/C-SiC (Si) composites with a SiC-based coating (not used in the present study) and actually sliding against materials of *different* composition (organic or metallic pads)[20, 21]. To conclude, we believe that C/C-SiC model composites, properly engineered at a submicrometer scale, fabricated in a controlled and reproducible manner by P-CVI (from different carbon precursors to vary the microtexture of the pyrocarbon matrix) and followed by a suitable HTT, could well be materials of choice for a detailed and fundamental study of a property as complex as friction.

5. MISCELLANEOUS

Other well identified properties of non-oxide CMCs could also be improved through material design at a submicrometer scale, such as their thermal conductivity and their stability under nuclear radiations, which will be now briefly discussed.

Thermal conductivity is an important material property in applications where relatively thin structural components are submitted at high temperature to a heat flux in a perpendicular direction (through the thickness direction). Such is the case for combustion chamber in aerojet engines and cogeneration

gas turbines, as well as heat exchangers in nuclear reactors. Generally speaking, the thermal conductivity of SiC-ceramics is not very high (although it is much better than those of most oxide ceramics). It depends on the state of crystallisation and residual porosity. Further, it decreases significantly as temperature is raised. As an example, it is of the order of $\lambda_f = 8\ Wm^{-1}\ K^{-1}$ for the SiC+C poorly crystallised Hi-Nicalon fibers, $\lambda_f \approx 65\ Wm^{-1}\ K^{-1}$ for the stoichiometric microcrystalline Tyranno SA SiC fibers and $\lambda_f \approx 60\ Wm^{-1}\ K^{-1}$ for a dense SiC-matrix deposited by CVD. Hence, it could be of interest to introduce in the SiC-matrix of SiC/SiC composites, a secondary and highly conductive phase to tentatively increase their transverse thermal conductivity. This subject has been recently tackled through modelling, for a simple SiC/SiC composite, i.e. a single infiltrated fiber tow[22, 23]. The computation showed that introducing a 200 nm thick layer of anisotropic pyrocarbon (with the graphene layers parallel to the fiber surface) in the SiC-matrix significantly increases the transverse thermal conductivity. For a 1D-SiC (Hi-Nicalon)/SiC (CVI) composite with the matrix assumed to be fully dense, the gain was ≈ 20 and even 110%, depending on the microtexture of pyrocarbon However, it is not presently known whether the use of a (PyC-SiC)n multilayer (with for example, n = 10 ; e (PyC) = 20 nm and e(SiC) = 50 nm), in place of the 200 nm single PyC-layer, would be advantageous or not.

SiC/SiC composites, with more precisely a β–SiC (3C-polytype) matrix and stoichiometric β–SiC fibers (such as Tyranno SA), are attractive structural materials for components of nuclear reactors, on the basis of their refractoriness, mechanical/thermal properties at high temperatures and low residual radioactivity after irradiation. One of the key issues here is the interphase design, both pyrocarbon and BN being reported to display a poor compatibility with a neutron environment. It has been recently suggested to use $(PyC\text{-}SiC)_n$ multilayered interphases with a PyC-content as low as possible[24, 25]. The present study actually shows that the thickness of the PyC-layers still acting as mechanical fuse could be reduced to e(PyC) = 10 to 20 nm (depending on the surface roughness of the SiC-fibers and SiC-layers). Hence, the PyC-thickness presently used, namely, 50 to 300 nm, could be lowered with an expected improved stability in a neutron environment.

These two new examples, although not yet fully supported by a large data base, show again the potential of SiC-matrix composites designed at a submicrometer scale, for improving their thermal conductivity and their compatibility with neutrons at high temperature.

6. CONCLUSION

From the results and discussion presented in sections 2-5, the following conclusions can be tentatively drawn:

(i) There is a clear advantage from a fundamental standpoint in designing non-oxide fiber-reinforced, multilayered (and cellular) ceramic composites at a submicrometer scale, typically 10 – 100 nm,

(ii) P-CVD/CVI is an appropriate and flexible processing technique to fabricate, at least at the laboratory and pilot-plant levels, ceramic composites engineered at such a scale and displaying regular or graded composition and microstructure.

(iii) The oxidation resistance and consequently the in-service lifetime of non-oxide CMCs (either fiber-reinforced, laminated or cellular) in oxidizing atmospheres is improved by promoting a self-healing behavior, through the reduction in thickness of the oxidation-prone phases (the interphase or cell-boundary) and the introduction of secondary phases forming healing (fluid) oxides (such as boria, silica and their mixtures).

(iv) The friction properties of C/C composites can be tailored by introducing a hard phase, such as a carbide (and by extension a boride or a silicide), in the carbon matrix, in a controlled manner and at a submicrometer scale. The coefficient of friction is improved but it is, however, at the expense of the wear resistance.

(v) Other properties, such as the thermal conductivity of SiC/SiC and their stability under nuclear radiations could also be tailored and improved through a proper design of their constituents at a nanometer scale.

ACKNOWLEDGEMENTS

The authors acknowledge the contribution of M. Brendlé from CNRS-ICS, Mulhouse, to the tribological tests, J.M. Goyheneche to the modelling of thermal conductivity, A. Guette and F. Rebillat to BN-deposition and oxidation tests, as well as P. Dupel and F. Heurtevent for their pioneering work on the P-CVD/CVI of pyrocarbon and SiC. They also like to thank J. Forget and C. Duhau for the preparation of the manuscript.

REFERENCES

1. R. Warren, *Ceramic Matrix Composites*, Blackie, Glasgow, 1992.
2. K.K. Chawla, *Ceramic Matrix Composites*, Chapman and Hall, London, 1993.
3. R. Warren, in *Comprehensive Composite Materials* (A. Kelly and K. Zweben, eds. In Chief), Vol. 4 Carbon/Carbon, Cement and Ceramic Matrix Composites, Pergamon/Elsevier, Amsterdam, 2000.
4. W.J. Clegg, Layered ceramic structures, in ref. 3, Chap. 4.15, pp. 449-470.

5. D.B. Marshall, J.J. Ratto and F.F. Lange, "Enhanced fracture toughness in layered microcomposites of Ce-ZrO_2 and Al_2O_3", *J. Amer. Ceram. Soc.*, **74** [12] 2979-2987 (1991).
6. Y. Shigegaki, M.E. Brito, K. Hirao, M. Toriyama and S. Kanzaki, "Processing of a novel multilayered silicon nitride", *J. Amer. Ceram. Soc.*, **79** [8] 2197-2200 (1996).
7. P. Dupel, "Pyrocarbon pressure-pulsed CVD/CVI: application to thermostructural composites", *PhD Thesis*, n° 927, Univ. Bordeaux 1, May 24, 1993.
8. F. Heurtevent, "$(PyC\text{-}SiC)_n$ multilayered materials: application to interphases in thermostructural composites", *PhD Thesis*, n° 1476, Univ. Bordeaux 1, March 29, 1996.
9. F. Lamouroux, S. Bertrand, R. Pailler, R. Naslain and M. Cataldi, "Oxidation resistant fiber-reinforced ceramic-matrix composites", *Composites Sci. Technology*, **59** (1999) 1073-1085.
10. S. Bertrand, "Improvement of the lifetime of SiC/SiC composites with nanosequenced $(PyC/SiC)_n$ and $(BN/SiC)_n$ interphases", *PhD Thesis*, n° 1927, Univ. Bordeaux 1, Sept. 29, 1998.
11. R. Naslain, R. Pailler, X. Bourrat and G. Vignoles, "Processing of ceramic matrix composites by pulsed-CVI and related techniques", *Key Eng. Mater.*, **159-160** (1999) 359-366.
12. A. Fillion, "C/C and C/C-SiC composites for tribological applications", *PhD Thesis*, n° 2168, Univ. Bordeaux 1, January 13, 2000.
13. F. Langlais, "Chemical vapor infiltration processing of ceramic matrix composites", in ref. 3, Chap. 4.20, pp. 611-644.
14. L. Filipuzzi, "Oxidation of SiC/SiC composites and their constituents: experimental approach, modelling and influence on mechanical behavior", *PhD Thesis*, n° 593, Univ. Bordeaux 1, March 29, 1991.
15. L. Filipuzzi and R. Naslain, "Oxidation mechanisms and kinetics of 1D-SiC/C/SiC composite materials: 2- modelling", *J. Amer. Ceram. Soc.*, **77** [2] 467-480 (1994).
16. F. Lamouroux, "On the behavior of 2D-C/SiC composite material in oxidizing environment", *PhD Thesis*, n° 860, Univ. Bordeaux 1, December 8, 1992.
17. F. Lamouroux, R. Naslain and J.M. Jouin, "Kinetics and mechanisms of oxidation of 2D woven C/SiC composites: 2, theoretical approach", *J. Amer. Ceram. Soc.*, **77** [8] 2058-2068 (1994).
18. D. Kovar, B.H. King, R.W. Trice, and J.W. Halloran, "Fibrous monolithic ceramics", *J. Amer. Ceram. Soc.*, **80** [10] 2471-2487 (1997).
19. S. Baskaran, S.D. Nunn, D. Popovic and J.W. Halloran, "Fibrous monolithic ceramics: I- Fabrication, microstructure and indentation behavior", *J. Amer. Ceram. Soc.*, **76** [9] 2209-2216 (1993).

20. W. Krenkel, "C/C-SiC composites for hot structures and advanced friction systems", *Ceram. Eng. Sci. Proc.*, **24** [4] 583-592 (2003).
21. P.J. Blau and H.M. Meyer III, "Characteristics of wear particles produced during friction tests of conventional and unconventional disc brake materials", *Wear*, **255** (2003) 1261-1269.
22. R. Naslain, R. Pailler, X. Bourrat, J.M. Goyheneche, A. Guette, F. Lamouroux, S. Bertrand and A. Fillion, "Engineering non-oxide CMCs at the nanometer scale by pressure-pulsed CVI", Proc. HTCMC-5, *Ceram. Trans.* (to be published), (2004).
23. J.M. Goyheneche, G. Vignoles and O. Coindreau, "Thermal modelling of thermostructural composites", *Proc. Congres Français de Thermique*, (SFT-2004), Giens, May 25-28, 2004 (in Press).
24. T. Nozawa, K. Hironaka, Y. Katoh, A. Kohyama, T. Taguchi, S. Jitsukawa and L.L. Snead, "Tensile strength of chemical vapor infiltrated advanced SiC fiber composites at elevated temperatures", *Ceram. Trans.*, **144** (2002) 245-252.
25. T. Hinoki, E. Lara-Curzio and L.L. Snead, "Mechanical properties of high purity SiC fiber-reinforced CVI-SiC matrix composites", *Fusion Science and Technology*, 44 (2003) 211-218.

Discussion

W. Rieger: Have you assessed the influence of the elastic moduli and of the differences in mechanical properties on the behaviour of the multilayer composites?

R. Naslain: Yes and no. On the one hand, when we designed our $(X\text{-}Y)_n$ multilayered interphases (with X = pyrocarbon or BN and Y = SiC), we have systematically combined materials (X and Y) with different mechanical properties, i.e. X is a material with a low shear strength (to promote crack deflection and debonding) and Y a stiff ceramic (here, SiC). Further, we have noticed a direct relationship between the strength of SiC/SiC composites in tensile loading (in the non-linear stress-strain domain) and the composition of $(PyC\text{-}SiC)_n$ multilayered interphases, i.e. between the amount of the soft pyrocarbon replaced by stiff SiC. On the other hand, no systematic study has been done to quantify the effect of the mechanical properties of the interphase on the behaviour of the composites. This could be done for simple composites (such as 1D-SiC/SiC composites) through modelling, assuming that the mechanical characteristics of the elementary layers at the nm-scale are known.

V. Vikulin: What is the maximum operational temperature for materials based on silicon carbide with protection and what will be the strength after thermocycling when there could be appearance of cracking?

R. Naslain: The answer to the first part of the question depends on the nature of the atmosphere. If one assumes that the atmosphere is oxidizing and the oxidation regime passive, the maximum operational temperature of SiC-based composites might be close to 1500 °C (beyond this temperature, the silica protective scale starts to volatilize). The residual strength after thermocycling strongly depends on the efficiency of the coating or of the matrix. If both of them are self-healing, the microcracks which are formed in the material are sealed rapidly as soon as they propagate and the in-depth oxygen diffusion is slowed down. Under such conditions, the oxidation damage is limited to near the surface of the composite. Further, the residual strength of the composite will also depend on the HT-properties of the fibers (the best being those close to Si/C = 1 stoichiometry which have been fabricated at high temperature, typically 1800 - 2000 °C). Experiments on SiC/SiC and C/SiC composites show that their mechanical behavior in oxidizing atmosphere tend to be better at high temperatures (≈ 1200 °C) than at lower temperatures (≈ 600 °C) where the self-healing behavior is less efficient.